We are IntechOpen,
the world's leading publisher of
Open Access books
Built by scientists, for scientists

6,900
Open access books available

185,000
International authors and editors

200M
Downloads

154
Countries delivered to

Our authors are among the

TOP 1%
most cited scientists

12.2%
Contributors from top 500 universities

CLARIVATE ANALYTICS

BOOK CITATION INDEX

INDEXED

WEB OF SCIENCE™

Selection of our books indexed in the Book Citation Index
in Web of Science™ Core Collection (BKCI)

Interested in publishing with us?
Contact book.department@intechopen.com

Development of a Modular Biosensor System for Rapid Pathogen Detection

René Hanke, Nina Bailly, Philipp Demling,
Florian N. Gohr, Patrick Opdensteinen,
Michael J. Osthege, Markus Joppich,
Suresh Sudarsan, Ulrich Schwaneberg,
Wolfgang Wiechert and Lars M. Blank

Additional information is available at the end of the chapter

Abstract

Progress in the field of pathogen detection relies on at least one of the following three qualities: selectivity, speed, and cost-effectiveness. Here, we demonstrate a proof of concept for an optical biosensing system for the detection of the opportunistic human pathogen *Pseudomonas aeruginosa* while addressing the abovementioned traits through a modular design. The biosensor detects pathogen-specific quorum sensing molecules and generates a fluorescence signal via an intracellular amplifier. Using a tailored measurement device built from low-cost components, the image analysis software detected the presence of *P. aeruginosa* in 42 min of incubation. Due to its modular design, individual components can be optimized or modified to specifically detect a variety of different pathogens. This biosensor system represents a successful integration of synthetic biology with software and hardware engineering.

Keywords: quorum sensing, FRET, signal amplification, whole-cell biosensor, customized hardware, online image analysis, point of contact, synthetic biology, iGEM, *Pseudomonas aeruginosa*

1. Introduction

A prerequisite for countermeasures against opportunistic pathogens is their rapid detection [1, 2]. In contrast, conventional diagnostic methods often utilize time-consuming techniques such as microscopy and cultivation in different media [3] and bear the risk of false-positive

or false-negative results [4]. Traditionally, microbiological tests have hence been performed by trained personnel in stationary laboratories, because the complex instrumentation hinders transportation [5].

Established methods for detection and identification of pathogenic bacteria most commonly rely on PCR, culture, and counting or immunological techniques such as ELISA. PCR-based methods are extremely sensitive but require purified samples and hours of processing as well as staff trained in molecular biology. Immunological methods are similarly sensitive but often require costly analytes (e.g., labeled antibodies). For detailed information, such as sensitivity, please refer to the "Discussion and outlook" section. Another commercially available technique for pathogen detection is flow cytometry, which offers rapid, quantitative measurements of multiple parameters of individual cells. However, it is expensive and requires stable growth conditions for the organisms to allow reproducible results [6]. Considering these limitations, the need for rapid, specific, and inexpensive point-of-contact tests becomes apparent. Furthermore, these tests should be intuitive to conduct while providing the same or a higher sensitivity than traditional detection methods [1, 7].

Biosensors represent a promising approach for pathogen detection and have the potential to fulfill the aforementioned demands [7]. For example, biosensors offer advantages such as high specificity and sensitivity [6]. Increasing effort has been spent on the development of biosensors that allow for portable microbiological tests since the 1990s [6, 8].

A biosensor can be defined as an analytical device in which a biologically active component (e.g., an enzyme, antibody, whole cell) is immobilized onto the surface of a transducing element (electronic, optic, or optoelectronic), allowing the detection of target analytes in complex mixtures [9]. A typical biosensor comprises three main parts: the bio-recognition component, the interface, and the transducing element [10]. The biological component specifically recognizes the analyte, and the biochemical interaction is then converted into a quantifiable signal via the transducer [9]. The choice of the interface and immobilization technique depends on the selected biological element and transducer [10]. Based on the method utilized for signal transduction, biosensors can be roughly classified into four basic groups, namely, optical, mass, electrochemical, and thermal sensors [6].

Optical biosensors are particularly interesting for detection of pathogens because of their higher sensitivity than electrochemical biosensors. For example, optical biosensors based on surface plasmon resonance (SPR) are already commercially available in a portable format (Spreeta System, Texas Instruments). Drawbacks of this technique are comparably high costs and complexity requiring trained staff for operation [5].

2. The five key elements of the proposed biosensor

The present work provides proof of concept for a novel approach toward a cost-efficient, optical biosensor, which enables safe and simple detection of pathogens and does not require highly trained staff for operation. The detection system was designed for investigation of solid

surfaces, for example, to assess cleaning success in a hospital environment, which is receiving increasing interest [10]. This project was performed and has successfully competed in the International Genetically Engineered Machine (iGEM) competition 2014 [11].

The potential of the proposed system lies within the combination of biology and engineering as the development of biosensors is highly interdisciplinary [7]. Five key components, namely, biomolecular detection (I) with intracellular signal amplification (II) embedded into a two-dimensional sensor chip (III), a custom incubation device (IV), and automated image analysis (V), constitute the functional biosensor as displayed in **Figure 1**. In terms of the biological component, the present project comprised the genetic engineering of sensor cells (introduction of the amplifying reporter circuit in *Escherichia coli*) as well as the optimization of the interface and immobilization of the resulting sensor cells. The transduction element (hardware), a customized detection unit, and image analysis software for automated evaluation were developed.

As a model organism for demonstrating the biosensor's functionality, the well-studied opportunistic pathogen *Pseudomonas aeruginosa* [12] was chosen as it has become a major cause of nosocomial infections; about 10% of nosocomial infections in most European Union hospitals are currently caused by *P. aeruginosa* alone [13]. Additionally, this bacterium often acquires multiple drug resistances and is a threat to patients suffering from cystic fibrosis, severe burns, or immunodeficiency [14].

2.1. Quorum sensing in *Pseudomonas aeruginosa*

Bacteria have evolved complex systems to sense their environment. Quorum sensing (QS) networks present a way to synchronize behavior, such as bioluminescence, biofilm formation, sporulation, and the secretion of virulence factors, on a population-wide scale [15].

In QS systems of bacteria, an autoinducer (AI) is produced by one or more synthases and is secreted from the cell. The cell can in turn detect the autoinducers through receptors in the
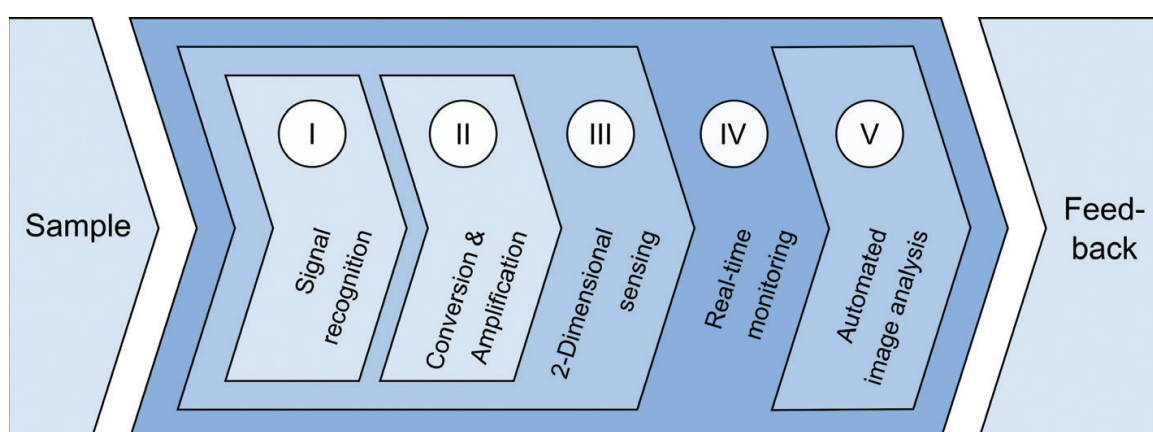

Figure 1. The five key elements of the proposed sensor system. A biomolecular signal originating from pathogens in the sample is recognized (I), converted, and amplified (II) by sensor cells embedded in a two-dimensional sensor chip (III). The chip is incorporated in a detection device capable of real-time monitoring (IV) and equipped with software for an automated image analysis (V). In combination, the setup gives feedback to the user if pathogens were detected.

cytosol (single-step response regulation in Gram-negative bacteria) or in the membrane (two-step response regulation in Gram-positive bacteria). Once a minimal threshold concentration is reached at higher cell densities, the activated AI receptors can induce or repress specific gene expression programs. The induction of the QS regulon leads to the expression of more AI synthase, amplifying the QS signaling [16]. However, most often the QS systems of one bacterial species extend beyond the basic circuit described above. Such configurations can include a multitude of circuits in parallel or series as well as competitive setups and on-off switches [17].

P. aeruginosa is commonly found in soil and is of particular interest due to its role in nosocomial infections. QS is essential for the persistence and disease progression, because it governs cell adhesion, biofilm formation, and virulence factor secretion [14]. The bacterium has three interconnected QS circuits: LasIR and RhlIR, two LuxIR-type circuits, and the *Pseudomonas* quinolone signal (PQS) system. In LasIR, the AI synthase LasI synthesizes the AI 3-oxo-C_{12}-homoserine lactone ($3OC_{12}$-HSL). LasR is a cytosolic receptor for $3OC_{12}$-HSL that acts as an inducer on the *las*I promoter once bound to the AI. LasR is only stable in the complex with its matching AI, in this case $3OC_{12}$-HSL. However, LasR not only activates the expression of the Las regulon; it also acts as an inducer for the transcription of *rhlR* and *rhlI*, the receptor and AI synthetase, respectively, in the second LuxIR-type QS system of *P. aeruginosa*. The interaction between the LasIR and RhlIR systems is illustrated in **Figure 2**. The details of *P. aeruginosa* QS have been described in literature [17, 18].

The implementation of the *P. aeruginosa* QS system in *E. coli* is already a well-established example for the use of such components in synthetic biology. Here, the LasIR circuit is used as a reporter system in *E. coli* to detect *P. aeruginosa*. The engineered *E. coli* cells constitutively express the protein LasR. Once $3OC_{12}$-HSL is secreted by *P. aeruginosa* cells, it diffuses into the *E. coli* cells and
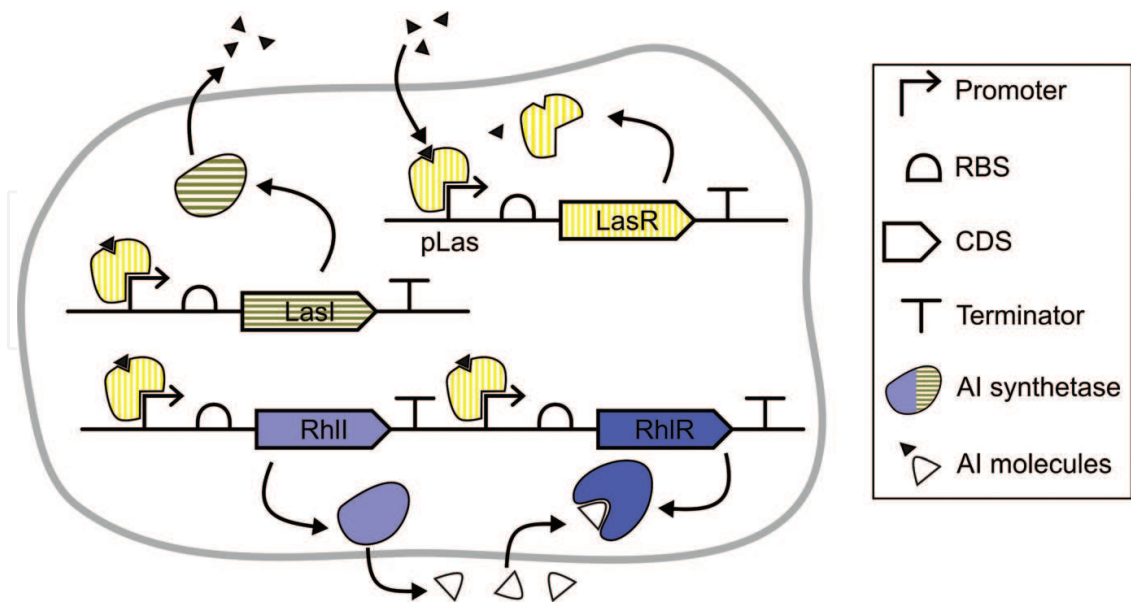

Figure 2. The LuxIR-type QS systems in *P. aeruginosa* and its translation into a biosensor. The AI synthase LasI (horizontal stripes) produces $3OC_{12}$-HSL (filled triangles) which bind to the transcription factor LasR (vertical stripes). The LasR-$3OC_{12}$-HSL complex induces the expression of the Las regulon as well as *rhlI* and *rhlR*. RhlI (light shade) synthesizes the AI C_4-HSL (open triangles) which in turn binds to RhlR (dark shade) and activates the expression of the Rhl regulon as well as the PQS system (not shown). RBS, ribosome binding site; CDS, coding sequence.

binds to LasR. The LasR-3OC$_{12}$-HSL complex then activates the reporter system, resulting in a fluorescent signal that can be read out by the detection device. However, the working principle of the biosensor is not limited to the detection of *P. aeruginosa*. Ultimately, the sensing *E. coli* cells can be engineered to include reporter circuits based on QS systems of other bacteria.

2.2. Molecular signal amplification

The biological component of the proposed biosensor was embodied by genetically modified *E. coli*, which were engineered to generate a fluorescence signal upon the presence of QS molecules specific for *P. aeruginosa* (specifically 3OC$_{12}$-HSL). The core component of the sensor cells is the activation of a pool of quenched fluorophores, which will be discussed in detail later. Desired properties of the sensor cells were a rapid response, specificity, and high sensitivity [10].

The traditional way to report the binding of 3OC$_{12}$-HSL to the constitutively expressed LasR would be the expression of a fluorescent protein, such as GFP, under the control of the *las*I promoter. The presence of the autoinducer would then lead to a detectable fluorescent signal. A rapid generation of the signal, however, would be limited by transcription, translation, folding, posttranslational modification, and maturation of GFP. Therefore, a novel reporter strategy to accelerate the signal generation was chosen. In the proposed system, a quencher-linked GFP fusion protein is constitutively expressed in the cells, but does not exhibit fluorescence as long as the quencher subunit is in close proximity to the GFP subunit. Binding of 3OC$_{12}$-HSL to LasR induces the expression of a tobacco etch virus (TEV) protease, which cleaves the fusion protein. Thereby, GFP is released from the quencher and emits a fluorescence signal. Compared to the conventional approach, the signal is generated faster by maintaining a stock of fusion proteins in the cells, which can be readily cleaved. Additional signal amplification is achieved by the ability of a single TEV protease to cut multiple fusion proteins, while expression of a fluorescent protein upon the presence of 3OC$_{12}$-HSL would only result in a single fluorescent molecule at a time.

2.2.1. Quenching of GFP fluorescence

The quenching of GFP fluorescence in the fusion protein is based on Förster resonance energy transfer (FRET), a process by which the energy of an excited donor fluorophore is transferred to an acceptor molecule whose absorption spectrum overlaps with the emission spectrum of the donor [19]. The energy can then be released, for example, by fluorescence of a longer wavelength or by heat. Yellow fluorescent protein (YFP) represents a suitable FRET acceptor for GFP. Emission resulting from YFP was avoided by using a nonfluorescent mutant of YFP called resonance energy-accepting chromoprotein (REACh [20]). Two REACh variants were generated by introducing the mutation Y145W (REACh1) and the double mutation Y145W/H148 (REACh2) into an enhanced YFP (eYFP) by QuikChange mutagenesis. Ganesan et al. [20] reported a reduction in fluorescence of 82 and 98% for REACh1 and REACh2, respectively.

Both REACh variants were genetically fused to GFP (mut3b [21]) via a linker, which brings both proteins in close proximity, facilitating FRET [22] from GFP to REACh, thus quenching the fluorescence. The linker harbors a cleavage site for the TEV protease (ENLYFQ\S) allowing the separation from the quencher. In the present study, the TEV protease is expressed under

control of the *las*I promoter, making it inducible by the QS autoinducer $3OC_{12}$-HSL. For this purpose, a TEV protease gene with codon optimization for *E. coli* and the anti-self-cleavage mutation S219 V was designed [23]. The GFP-REACh fusion protein is expressed constitutively to ensure continuous supply of protease substrate. **Figure 3** illustrates the interplay between the GFP-REACh fusion protein and the TEV protease. The expression cassette for the GFP-REACh fusion protein was cloned into a pSB3K3 [24] vector backbone, and the TEV protease expression cassette was inserted into a pSB1C3 [25] vector.

2.2.2. Validation of the reporter system

For initial validation the developed reporter system was tested via β-D-1-thiogalactopyranoside (IPTG) induction using a well-characterized T7 promoter instead of the *las*I promoter. Two plasmids, one carrying the GFP-REACh fusion protein and one carrying the TEV protease, were introduced into *E. coli* BL21 (DE3). The resulting strain allowed the IPTG-inducible expression of the fusion protein. A growth experiment was conducted in which the fluorescence of the double plasmid strains, containing either variant of the fusion protein and the TEV protease, was compared to cells constitutively expressing GFP as positive control and a nonfluorescent strain as negative control (**Figure 4,** left). For both REACh variants, IPTG-induced as well as IPTG-non-induced cultures were grown in parallel, and all measurements were done in a biological triplicate. The fluorescence was normalized to the observed optical density (OD). The induction with IPTG leads to a rapid increase of the fluorescence signal. At the end point, a signal strength comparable to the positive control was reached, indicating a complete cleavage of the fusion proteins by the TEV protease. The higher base level of fluorescence in the non-induced cells can be attributed to imperfect quenching. This experiment demonstrated the quenching ability of the REACh proteins in our fusion constructs as well as the functionality of the *E. coli*-produced TEV protease.
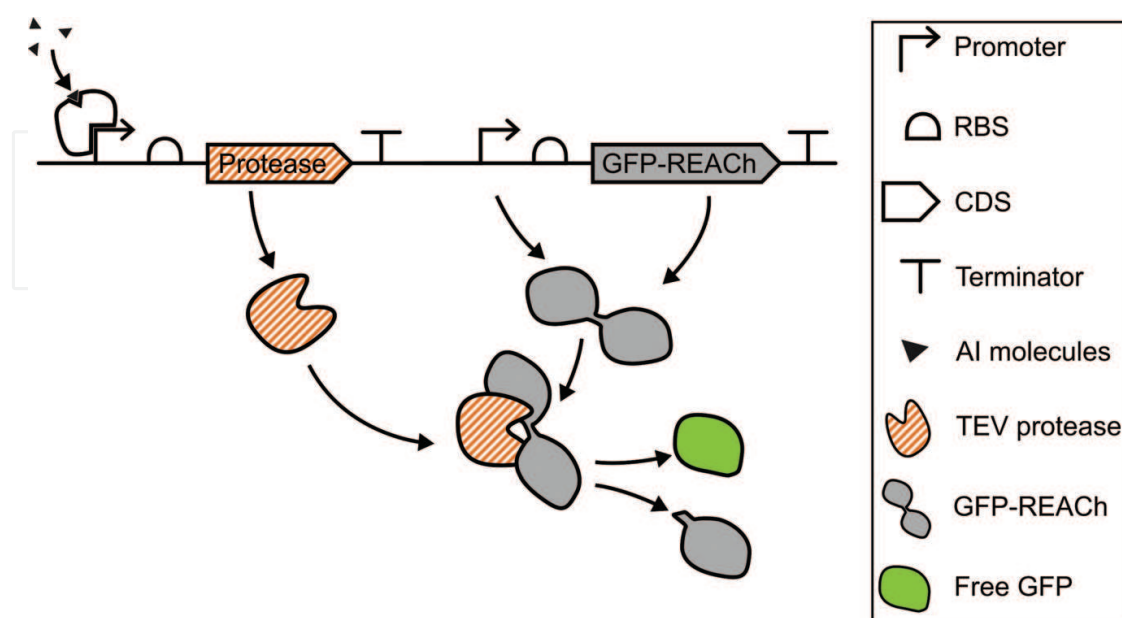

Figure 3. Schematic model of the novel biosensor. Expression of the TEV protease is induced by bacterium-specific HSL bound to its receptor LasR. The protease then activates a pool of readily available fluorophores by cleaving off the quencher (REACh) and releasing fluorescent GFP. RBS, ribosome binding site; CDS, coding sequence.
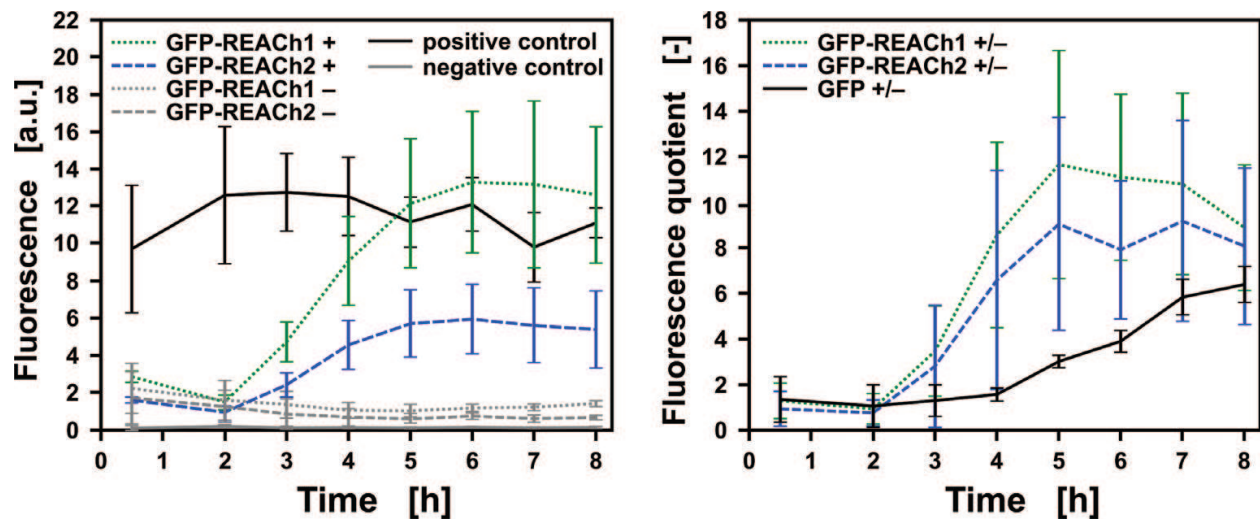
Figure 4. Validation of the reporter system. The production of a fluorescence signal by REACh variants after protease cleavage was compared. Each variant was tested with and without IPTG induction. Constitutive GFP expression and a nonfluorescent strain were used as positive and negative controls, respectively. The fluorescence signal was normalized by the sample OD (left). Comparison of response time of the biosensor setup to conventional GFP expression. The expression of all three systems was under the control of the IPTG-inducible lacI promoter. The fluorescence signal was normalized by the sample OD and based on the signal of a negative control (right). Error bars represent errors as determined by Gaussian error propagation using standard deviations from three biological replicates.

To test the hypothesis that the GFP-REACh fusion proteins in combination with the cleavage amplification results in a faster response than the conventional approach, the kinetics of our reporter strategy were compared to a strain expressing GFP under the control of an IPTG-inducible *lac*I promoter. Using the new reporter strategy, a much stronger and faster increase in fluorescence was observed compared to IPTG-induced expression of GFP (**Figure 4,** right). The high variation for the development of fluorescence by the GFP-REACh systems may have originated from inhomogeneous expression levels of the TEV protease and different sizes of the fluorophore pools. As the signal is amplified by the cleavage of the GFP-REACh fusion protein by the TEV protease, even slight temporal differences in the expression of the TEV protease are expected to cause great shifts in the temporal signal responses, thus resulting in high error bars when different cultures are averaged. The errors were increased even further with the Gaussian error propagation.

2.3. Immobilization of sensor cells

The sensor cells were immobilized in rectangular layers (chips), thus creating an interface between the biological component and the technical component (transducer). Main objectives during the design of the interface were to enable viability and storability of the immobilized sensor cells, reproducibility of the fluorescence response, as well as cost-efficiency. For proof of concept, a simple and robust design was chosen.

A variety of different methods have been used for immobilization of whole cells, which can be divided into six general types: covalent coupling, affinity immobilization, adsorption, confinement in liquid-liquid emulsion, capture behind semipermeable membranes, and entrapment [26]. An established technique for immobilization of living cells is entrapment, which refers to the physical containment of organisms inside a matrix or fibers, thus creating a protective

barrier around the cells [27]. Matrices used for entrapment can be synthetic polymers, such as polyester, or natural polymers, such as agar, agarose, or alginate [27]. Entrapment allows to preserve and prolong cell viability, for example, during storage [26, 27], which matched the intentions of this work.

Important prerequisites for the entrapment matrix of the sensor cells were physical rigidity, safety, resistance against biological degradation, transparency, as well as the possibility to conduct matrix synthesis at mild conditions, suitable for living cells. Inorganic polymers such as polyacrylamide were ruled out due to the carcinogenicity of the monomers and rather harsh polymerization conditions [28]. Natural polymers allow for higher diffusion rates than inorganic polymers (tested for small molecules [28]) and are less expensive and less hazardous in production than synthetic polymers. The organic polymer agarose offers several advantages including easy handling, resistance to microbial degradation, and favorable conditions for entrapped cells [27]. Thus, agarose was the polymer of choice for immobilization of cells and formation of chips.

2.3.1. Optimization of chip casting mold and medium

First, a casting mold for rapid and reproducible manufacturing of the 2D sensor chip was developed. A plain surface was a prerequisite for automated image evaluation. Low agarose concentrations (<3.0%) were chosen to reduce consumable costs and to ensure rapid diffusion of the analyte (HSL) to the immobilized sensor cells.

Manufacturing of the agarose gel was conducted based on existing protocols for entrapping living cells in melted polymers. In brief, the temperature of the polymer solution was adjusted to 45°C and was quickly poured into the respective mold after mixing with the sensor cells. Sensor cells were spun down from a liquid culture (50 mL LB, 5 g·L^{-1} NaCl, 10 g·L^{-1} tryptone, 5 g·L^{-1} yeast extract) and resuspended in 1 mL LB medium (21°C) before mixing with the temperature-adjusted agarose solution, resulting in a cell concentration of approximately 5.6×10^9 cells/mL. Before usage, solidified and cutout sensor chips were incubated for 1 h at 37°C.

An open casting mold, which exploited the surface tension of the polymer solution to achieve a plain chip surface, was most successful for the production of sensor chips. After discarding a small gel area in direct contact with the edges of the mold (**Figure 5**, left), bubble-free sensor chips with a plain surface were readily obtained from this approach. The open mold allowed for simple, reproducible, and rapid manufacturing of sensor chips and was hence the method of choice for this work. An agarose concentration of 1.5% was found to be sufficient to cast robust sensor chips. For an accelerated manufacturing process, multiple sensor chips were casted simultaneously using an extended mold (**Figure 5**, left).

Further, to meet the nutritional needs of the sensor cells while minimizing background fluorescence, different complex media (Luria-Bertani or LB medium, Terrific-Broth or TB medium, nutrient agar or NA medium) as well as minimal media (Hartmans minimal or HM medium, M9 minimal medium) were tested with respect to sensor cell growth and the presence of background fluorescence. Background fluorescence was investigated in a commercial gel imaging system (GelDoc™ XR, Biorad, Germany) as well as in the custom-made optical detection device constructed in this work as described in the following section. The results are summarized in **Table 1**, and a comparison of the background fluorescence
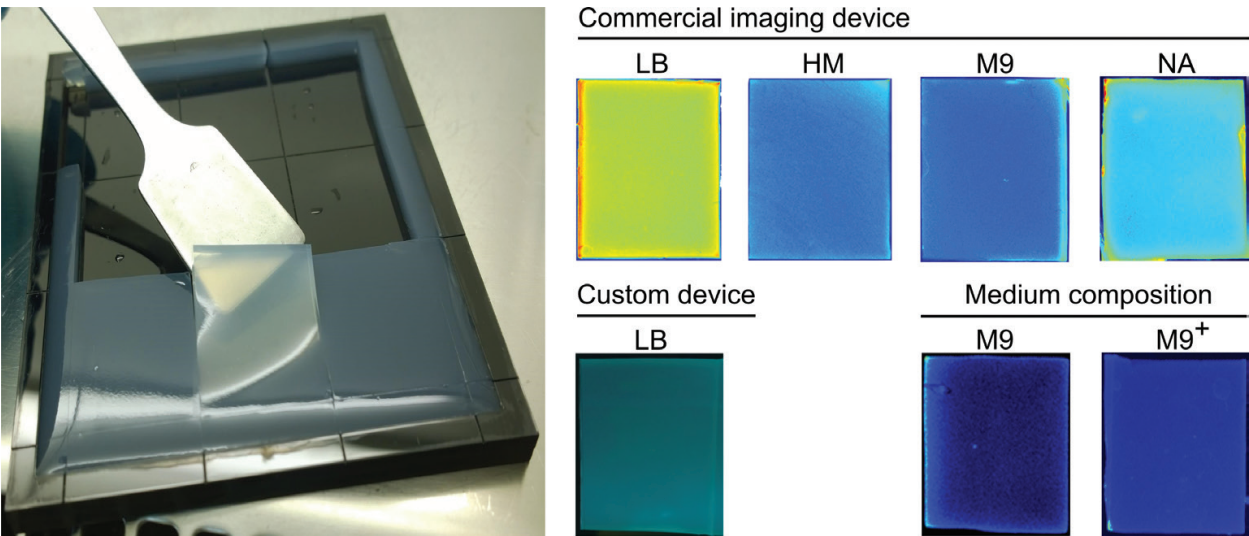
Figure 5. Sensor chip manufacturing and optimization. Sensor chip manufacturing (left) and effect of the medium choice on background fluorescence (right). M9⁺ represents supplementation of the M9 minimal medium with Casamino acids. Excitation commercial gel imaging system and in the custom-made optical detection device was conducted at 480 nm. Chips displayed contained 1.5% agarose and no sensor cells.

of sensor chips comprising the respective media is displayed in **Figure 5** (right). Only LB medium allowed for sufficient growth of the sensor cells. Its background fluorescence in the custom-made optical detection device was acceptable, most likely due to the narrow excitation profile compared to the commercial device.

Background fluorescence appeared to be more intense in complex media than in minimal media. To identify a possible cause for this observation, minimal M9 medium was supplemented with 2% Casamino acids (**Figure 5**, right, bottom row). Background fluorescence was stronger in supplemented minimal medium matching reports in literature [29], possibly due to an increased concentration of aromatic amino acids possessing inherent fluorescence.

Activity of the sensor cells after immobilization was investigated in a subsequent experiment by inducing a fluorescent signal with 0.2 μL of a 500 μg·mL⁻¹ HSL (3-oxo-C_{12}) solution (**Figure 6A**).

	Luria-Bertani medium	Terrific-Broth medium	Nutrient agar medium	M9 minimal medium	Hartmans minimal medium
Growth of sensor cells	+	+	—	—	—
BF, gel imaging system	—	—	+	+	+
BF, custom-made device	+	—	+	+	+

Fluorescence in the commercial gel imaging system and in the custom-made device was measured at λ_{ex} = 480 nm. Growth in the respective media was investigated in liquid culture; background fluorescence was investigated in chips containing 1.5% agarose and no sensor cells. + indicates either growth of the sensor cells or the absence of background fluorescence (BF); − indicates the absence of growth or the presence of background fluorescence.

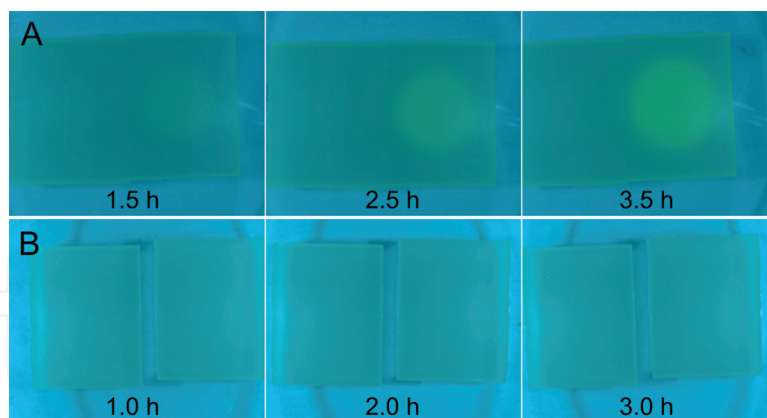**Table 1.** Compatibility of different growth media with the proposed 2D biosensor.

Figure 6. Assessment of the sensor cell viability after immobilization. (A) Fluorescence was induced with 0.2 μL of a 500 μg·mL⁻¹ HSL (3-oxo-C$_{12}$) solution. (B) a non-induced negative control was included to ensure that observed fluorescence only originated from induced sensor cells. Pictures were taken with the custom-made device (λ_{ex} = 480 nm) at different times after induction. Sensor chips were prepared as described in the text section and incubated for 1 h at 37°C before induction.

One and a half hours post induction, a fluorescence signal was visible even to the naked eye, indicating that the sensor cells were in fact still viable after immobilization. No apparent change in fluorescence was observable for the negative control (**Figure 6B**).

For easier handling and experimentation, storability of the sensor chips of several days was desired. Activity of the immobilized sensor cells after storage under different conditions was investigated by induction with HSL. Generation of a fluorescence signal was used as an indicator for cell viability. After storage at −20°C, no fluorescence was observed after thawing and inducing the sensor chips. The addition of glycerol in different concentrations (5–10% v/v) did not improve cell survival at −20°C. The shelf life at 4°C was 5 days, allowing a batch-wise production and storage for later use. Exceeding this storage duration led to an insufficient fluorescence response upon induction.

Additional experiments were carried out to investigate the biosafety of the proposed sensor chips, because a release of the genetically modified sensor cells from the sensor chips represented a possible risk in handling. A simple approach for investigating the biosafety of the sensor chips was replica plating on agar plates containing the respective antibiotic. An average of five colony-forming units (CfU) was found (n = 3), indicating that some cells were in fact able to escape the agarose entrapment. Therefore, measures to achieve a complete entrapment, for example by increasing the agarose concentration, should be evaluated to render the system as safe for the use in non–GMO-certified areas.

2.4. Integrated cultivation and detection device

The two-dimensional approach of sensing pathogens on agarose chips requires a specialized device for detecting and interpreting the fluorescent signals generated by the immobilized sensor strain. Since the results from commercially available plate readers and gel imaging systems did not yield a sufficient spatial resolution, a custom-made device was designed and constructed as pictured in **Figure 7** (left).
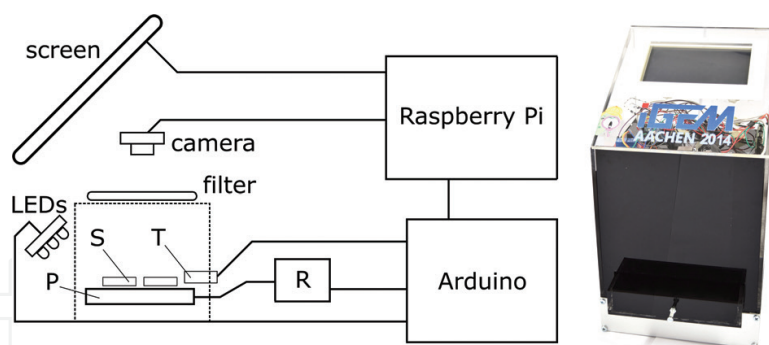
Figure 7. Schematic representation of hardware components and assembled device. Biosensor chips (S) are placed above a Peltier heating element (P) in the incubation chamber (dotted line). An Arduino microcontroller measures the temperature (T) and switches the heating on or off via a relay (R). A Raspberry Pi microcomputer displays the graphical user interface with the analysis software on the touchscreen. Whenever a picture is taken, the two controllers communicate to switch the excitation LEDs on/off. The fully assembled device (right) is sprayed black to avoid interference of ambient light. Stickers of the project logo are visible at the top.

The device consists of two enclosed compartments, separated by laser-cut plates of acrylic glass. The inner compartment serves for cultivation and illumination of the sensor chip. The outer compartment contains a Raspberry Pi microcomputer, an Arduino microcontroller, and a camera for imaging. **Figure 7** (right) schematically shows the individual components of the device and their interaction.

Once the chip is prepared and a sample taken, a petri dish containing the chip is inserted into the inner compartment, which serves as an *in situ* incubation chamber for both pathogens and genetically modified sensor organisms. A UV lamp could be integrated to facilitate built-in inactivation of microorganisms.

During the experiment, the parameters are controlled by an Arduino Uno and a Raspberry Pi. The Arduino has two main functions: first, it is responsible for controlling the incubation temperature in the inner compartment. Based on measurements from the temperature sensor, it sets the power input for the Peltier elements, thus heating or cooling the interior of the device. Second, the Arduino controls the LEDs illuminating the chip. When a control command from the Raspberry Pi is received, the two channels of the connected relay are turned on or off, switching the state of the LEDs, respectively. Thus, the chip is exposed to the specific wavelength emitted by the LEDs, in this case 480 nm for the excitation of the unquenched GFP.

Upon user input, the Raspberry Pi triggers the camera module to take an image of the chip. A filter slide is placed in front of the lens to block the excitation wavelength from the LEDs and to specifically transmit the emission wavelength of the fluorophore. In this configuration, a highly resolved fluorescent signal is obtained. The image is further processed by the Raspberry Pi and displays the analysis results via the graphical user interface (GUI) on a built-in 7-inch display located in the outer casing. The GUI (**Figure 8**, left) runs on either the Raspberry Pi or an externally connected computer; it enables the user to adjust the camera settings, take a single image or start time-lapse imaging, and to monitor the imaging process. Moreover, it allows execution of the analysis software for saved images as described in detail
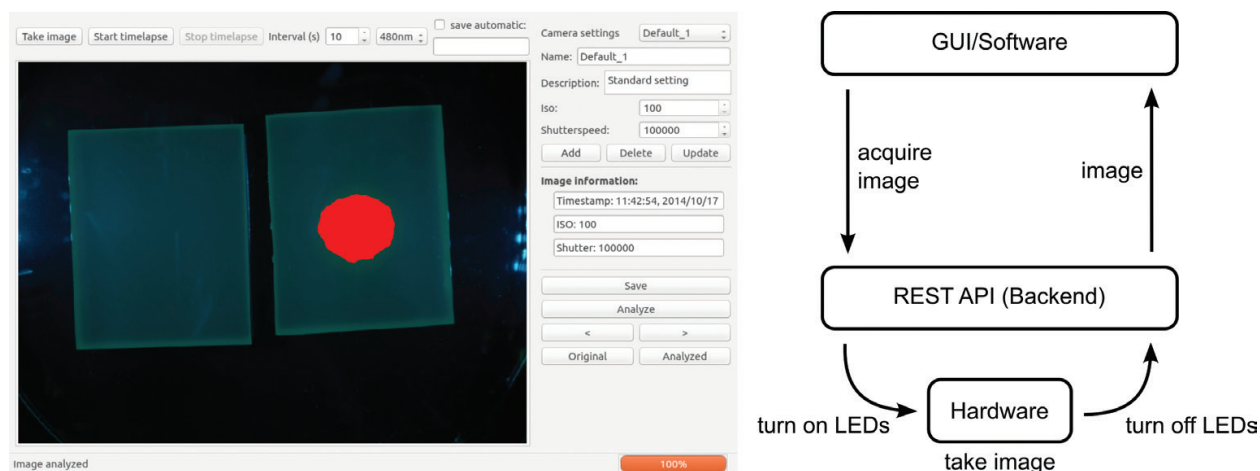
Figure 8. Graphical user interface (GUI) and chain of commands. Using the GUI (left) the user can specify settings for cultivation and imaging. The software instructs the backend via a REST API (right) to execute the imaging command. The acquired image is transferred back to the software which performs an automated analysis.

below. The communication between the GUI and the hardware is ensured by the backend software. It receives the respective commands (e.g., for capturing an image) from the GUI and subsequently forwards them to the according hardware. Therefore, the backend is responsible for image acquisition. An exemplary chain of commands for taking an image is depicted in **Figure 8** (right). The backend runs on the Raspberry Pi.

For the detection of *P. aeruginosa* using the sensor system presented in the previous sections, time-lapse imaging was performed, taking pictures in intervals of 5 min. The agarose chip was incubated at 37°C and excited with four LEDs (Superflux LED blue 3 lm NSPBR70BSS-PU/PV-W, Nichia Corporation) emitting a peak wavelength of 480 nm. The filter "010 Medium Yellow" (LEE Filters) was installed in front of the camera to allow the emission wavelengths of the fluorophore to pass while blocking the peak wavelength of the LEDs.

2.5. Analysis of spatial fluorescence

Automated, fast, and reliable analysis of raw sensor data is critical for a diagnostic device. Since, in the case of the 2D biosensor, the raw sensor measurement is a series of pictures taken by the onboard camera, an image analysis pipeline is required. Here, a novel pipeline is presented involving segmentation through statistical region merging (SRM [30]), thresholding in hue-saturation-value (HSV)-color space, and a final classification step. This leads to segmentation of the fluorescent regions in the biosensor chip, thus identifying chips or chip regions containing pathogens.

2.5.1. Image segmentation

Onboard image analysis on embedded computing hardware is subject to rigorous performance constraints due to the poor availability of existing analysis packages and the limited computing power. This complicates the use of sophisticated analysis pipelines. At the same time, the need for quantification of fluorescent regions on the biosensor mandates the image to be segmented into foreground (fluorescent) and background regions, also called super-pixels. This is necessary because only after a segmentation mask is computed for an input image, the number of

independent fluorescent regions in the image, their intensity, and their area can be quantified. Statistical region merging is an image segmentation algorithm which is both light-weight and does not require expensive tuning of algorithm-specific hyperparameters [30]. In contrast to other clustering algorithms, it also produces deterministic results, which increases the reproducibility of the analysis pipeline. The SRM algorithm has one important hyperparameter Q which influences the merging process. A Q-level of 256 resulting in many fine regions was chosen (**Figure 9**, top-left).

The input image (**Figure 10A**) is segmented into super-pixels, and the list of regions is filtered to obtain only candidate regions of fluorescence (**Figure 10B**). Since the color of the fluorescence signal is known, the regions can be thresholded based on their HSV color representation. For selection of GFP-fluorescent regions, super-pixels that have hue (color shade) in the interval [0.462, 0.520], saturation of 0.99, and value (brightness) in the interval [0.25, 0.32] were considered. This thresholding step removes background regions and is performed at low computational cost (**Figure 10C**).

Since false positives can remain after filtering, they are removed from the list of candidate regions by classifying each region into noise or signal. First, the classification applies a smoothing procedure to the region mask. This is achieved by convolving the region mask with a disk filter (**Figure 10D**). Then, for each pixel p' in that smoothed image, the smoothness index [31] is calculated (**Figure 10E**) as the sum of the difference with respect to each of its neighbors N_k (**Eq. (1)**). In the implementation, the neighbors in a radius of i=4px were used. Finally, the matrix of smoothness indices is normalized the interval [0, 1]:

$$S_p = \frac{\sum_{p' \in N_k} \nabla(p')}{\max_p S_p} \tag{1}$$

A subsequent thresholding step selects pixels that fulfill $S_p \geq T_S \wedge I_p \geq 255$ where S_p denotes the smoothness index at pixel p, T_s=0.85 is an empirically determined smoothness threshold, and I_p is the intensity of the pixel in the smoothed mask. The final classification step removes regions with high-edge curvature and selects smooth, blob-like regions (**Figure 10F**). Thereby, artifacts are removed from the analysis, and only fluorescent pixels are quantified.
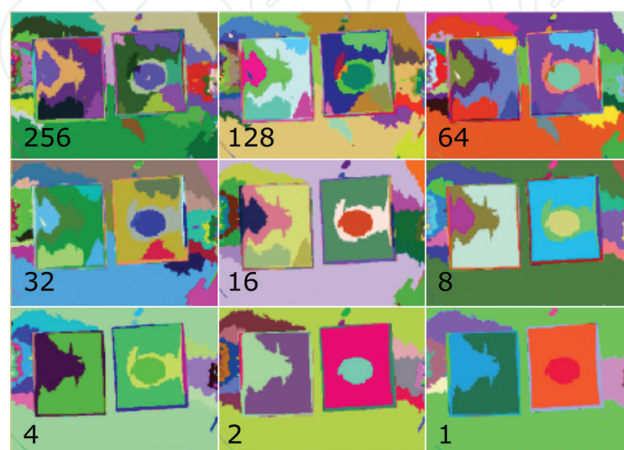

Figure 9. Regions obtained from SRM with different Q-levels. High Q-levels (indicated by numbers) result in many super-pixels (top-left), while low Q-levels correspond to rigorous merging (bottom-right). Segmented regions are randomly colored for better visualization.
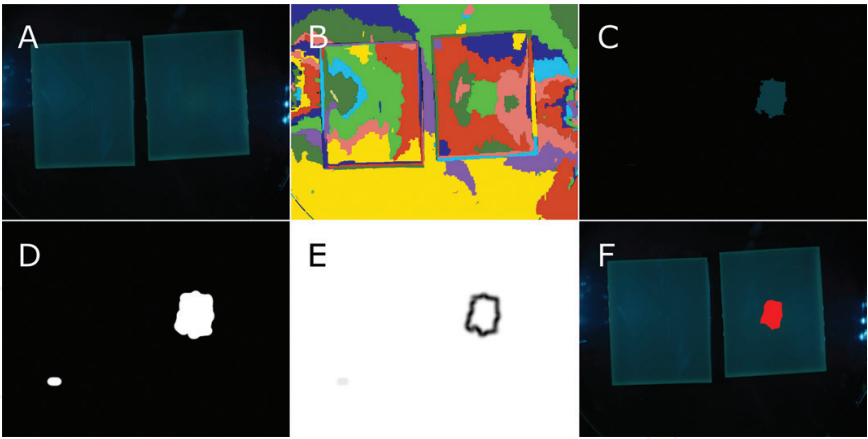
Figure 10. Input, intermediates, and result. The input image (A) is segmented using statistical region merging (B), and super-pixels are selected based on the HSV properties (C). The binary region mask is smoothed (D), and smoothness indices are computed (E). Pixels that were classified as foreground in D and smooth (E) are overlaid as red pixels on the input image (F).
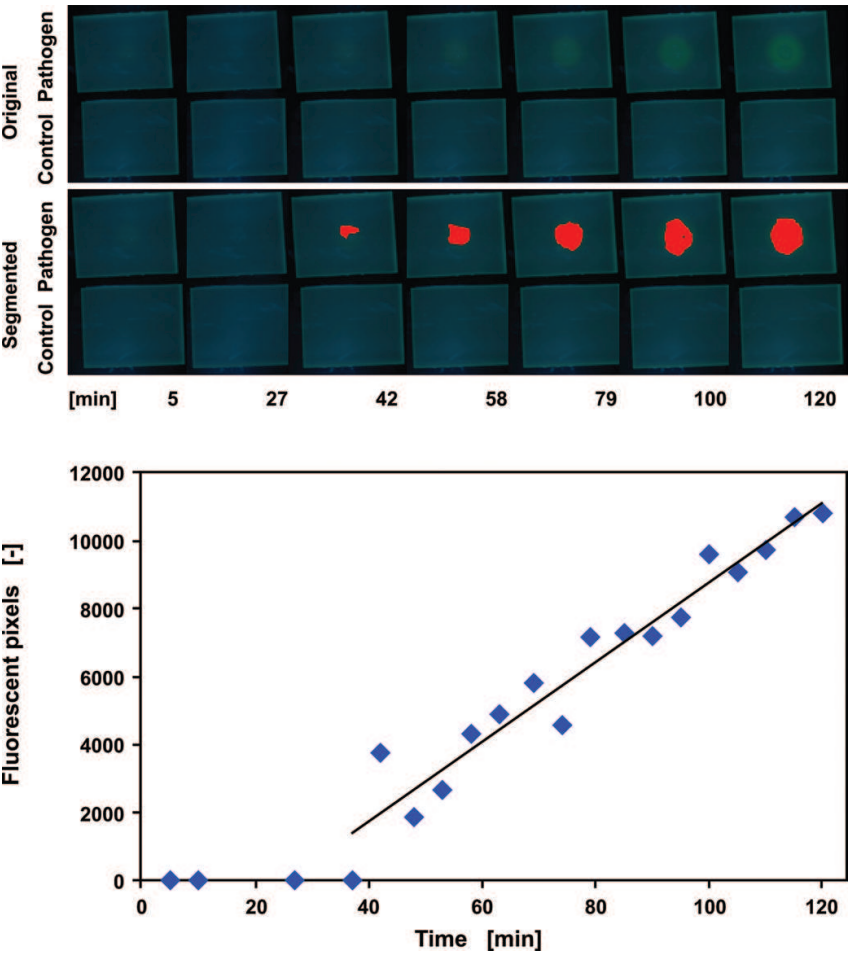

Figure 11. Time series acquired by the measurement device and quantification of fluorescent pixels over time. A volume of 0.2 μL of bacterial culture in LB medium (approximately 6×10^5 CFU) was added onto the center of agarose chips containing the immobilized sensor cells. The negative control culture contained *E. coli* DH5α, the pathogen sample culture *P. aeruginosa* O1. The chips were incubated at 37°C, and pictures were taken approximately every 5 min. The fluorescence signal recognized by the image analysis software is shown as highlighted area. A video sequence of the live pathogen detection can be found at [32] (top). A time series of images taken with the measurement device was analyzed using the outlined image analysis pipeline. Counts of foreground pixels (dots) are plotted against incubation time. Starting after 40 min of incubation, the number of fluorescent pixels linearly increased (117 pixels/min, $R^2 \approx 0.936$; bottom).

2.5.2. Quantification of the fluorescence signal

The image analysis pipeline outlined above was implemented in both MATLAB and C++. It allowed the detection of fluorescence with little tuning of hyperparameters (*Q*-level and thresholds). When a time-lapse of images is automatically acquired with the software, the image analysis pipeline can be applied to each frame (**Figure 11**, top). The number of pixels in the resulting foreground regions can be quantified over time. After about 40 min of incubation, a region of pathogen-induced fluorescence was detected, which then grew linearly with respect to its area over time (**Figure 11**, bottom). As a proof of principle, 6×10^5 cells were applied on the chip. However, serial dilution testing is needed to determine the lower detection limit. The expected lower limit of detection is 1 CFU due to cell proliferation during the incubation step.

3. Discussion and outlook

In this work, a modular biosensor for the detection of the opportunistic human pathogen P. aeruginosa was developed. Five key components, (2.1) a selective molecular detection mechanism, (2.2) an integrated amplification step, (2.3) a gentle immobilization technique, (2.4) a low-cost cultivation and optical detection device, and (2.5) a graphical analysis software, were integrated. The resulting modular biosensor demonstrates the power of combining synthetic biology with software and hardware engineering by detecting P. aeruginosa in less than 1 h of analysis time. **Table 2** provides a comparison of the sensor system developed in this study to existing detection methods for P. aeruginosa.

In addition to the detection methods compared in **Table 2**, there are several whole-cell approaches. Most of the previously developed whole-cell biosensors deliver an optical output [39]. In a previous work, Struss et al. developed a whole-cell biosensor detecting AHLs of gram-negative bacteria, particularly *P. aeruginosa* [40]. Similar to the approach presented herein, they used components of the AHL-mediated QS regulatory system to generate an optical signal. A portable format was developed by liquid-drying the sensor cells on filter paper strips. While Struss et al. met many criteria for a successful portable on-site field kit, such as easy handling, inexpensiveness, and simple transportation, it lacks a rapid, integrated analysis and is dependent on the user's subjective evaluation.

Enhancement and optimization of the proposed biosensor system beyond the proof of principle demonstrated in this work can be realized by modifying each of the five key elements as well as their interactions. The individual key elements can be optimized as follows.

The utilization of the pathogen's inherent QS system guarantees a high specificity as the receptor for the AI is unique. However, this poses a challenge if multiple pathogens are desired to be detected simultaneously. First, only QS molecules can be recognized by a molecular sensing system of the presented type. In theory, other secreted compounds can be used for detection, though potentially reducing the specificity. Second, the sensing system should be introduced into a separate sensing organism to completely avoid interaction, especially if a closely related QS system and a signal amplification as presented here are utilized. This may lead to insufficient spatial resolution as many different sensing cells are required to be incorporated in the same sensor chips. An equal distribution of each type of sensing cell needs

Principle of detection	Details	Advantages	Disadvantages
PCR	Targeting *gyrB* gene using real-time PCR, sensitivity: 3.3×10^2 to 2.3×10^3 CFU/PCR [33]	High selectivity and reliability, conclusive and unambiguous results, fast compared to culturing methods	No discrimination between viable and nonviable cells, purification step required
Culture and colony counting	Simple and traditional plating method, sensitivity: 20 CFU/mL [34]	Moderate selectivity, simple, inexpensive, low detection limit	Time-consuming cultivation of several days, detects only viable/culturable organisms, unspecific
Immunology	ELISA applying antibodies to detect cell surface antigens [35], typical sensitivity: 10^6 CFU/mL [6]	High selectivity, faster than PCR-based techniques	Complex and expensive, less sensitive than PCR, regularly requires cultural enrichment
Modular biosensor presented in this study	Transcription factors recognize pathogen-specific quorum sensing molecules; signal is transduced through activation of quenched fluorophores, tested number of cells: 6×10^5 CFU	Inexpensive (no expensive reagents or equipment required), rapid (short cultivation without pretreatment), simple (no highly trained personnel required)	Selectivity and sensitivity dependent on detection system, viable cells required
Nucleic acid biosensor	Reception through (-)ssDNA probe coupled to piezoelectric transduction, sensitivity: 0.1 µg/mL [36]	Detection in under 3 h, high selectivity	Low sensitivity, complex immobilization on hybrid membrane
Molecular imprinting polymer-based biosensor	Recognition of bacterial structure in combination with dielectrophoresis, sensitivity 10^3 CFU/mL [37]	Detection time of 3 min, high sensitivity, no pretreatment necessary	Cross-reactivity with bacteria of similar shape
Droplet-based microfluidic biosensor	Detection of virulence factors via surface-enhanced Raman spectroscopy, sensitivity: 0.5 µM pyocyanin [38]	Low sample volume, low detection limit for pathogen-specific virulence factor pyocyanin	Expensive, trained personnel required, increased technological effort, fluid samples only, extensive interpretation of data needed

Table 2. Conventional methods and biosensor approaches for detection of *P. aeruginosa*.

to be ensured and reciprocal interference avoided. The feasibility hereof has already been proven in previous work [41].

By introducing the REACh quenching system, the fluorescence response was amplified and accelerated compared to conventional GFP expression. Quenched fluorophores are constitutively expressed, and a constant pool of reporter molecules is built up. Upon the presence of inducers and a subsequent expression of the protease, they are unquenched resulting in a fast and strong fluorescent signal. Since the two expression cassettes for the GFP-REACh fusion protein and the TEV protease are currently on two separate plasmids, using a single plasmid would increase the robustness of the detection system, as two plasmid expression systems are considered less stable. As a proof of principle, the system was tested using IPTG-induced expression of the TEV protease. As a next step, the system would be adjusted by exchanging the T7 promoter with the HSL-bound LasR-inducible *las*I promoter to render the expression of the TEV protease

inducible by $3OC_{12}$-HSL. Subsequently, extensive testing with different concentrations of $3OC_{12}$-HSL and varying cell numbers of *P. aeruginosa* should be performed to determine detection limits. Based on the results, the expression can be fine-tuned, for example, by improving the promoters. On the protein level, the linker length between GFP and REACh can be optimized with respect to the protein folding, protease accessibility, and quenching efficiency [22].

Engineering of the agarose chips for entrapment of the sensor cells represents a simple yet efficient way for a two-dimensional detection method. The immobilized sensor cells survived and still performed as expected, even after short-term storage at 4°C. A fluorescence signal was generated upon induction, thus proving a sufficient diffusion of the inducer through the chip. As discussed above, adjustment of the agarose concentration used for production of the sensor chips represents a simple way to further optimize the sensor chips. Increasing the agarose concentration could focus the fluorescent response on a smaller area by restricting diffusion of the analyte, however, under the prerequisite that the diffusion is fast enough to reach the sensor cells within a short time. Additionally, adjustment of the agarose concentration affects the biosafety as the ability of the chip to contain the sensor cells is altered. To ensure a sufficient quantity and spread of the cells, an array-based technique for pattering the sensor cells onto a chip surface could be used to enable high-throughput analysis [41]. Several techniques for printing bacteria on surfaces have already been used successfully [42, 43].

The optical detection device represents a simple and cost-effective solution for the rapid visualization and analysis of the 2D fluorescent signal. In situ cultivation with automatic, real-time monitoring of the fluorescence resulted in the detection of *P. aeruginosa* within 42 min, even without using the optimized sensor cells. Compartmentation and the possibility to install a UV sterilization light ensures a high standard of biosafety. The settings described in Section 2.4 are highly specific for the presented two-dimensional biosensor; however, as the device is modular, single components such as the LEDs and the filter sets can be exchanged to adjust the optical settings to different reporter systems. An extension of the device, for example, by using a filter wheel or a monochromator and LEDs emitting different wavelengths bears the potential of simultaneously detecting various pathogens if respective molecular reporter systems can be constructed, thus allowing a high degree of multiplexing. The extensive modularity and the inexpensive parts in comparison to common commercial devices grant an easy access for potential users and researchers customizing the system for other biosensors.

The analysis software pipeline recognized and distinguished fluorescent signals of certain shapes and marked them for an easy interpretation by the user. However, the lack of sufficient amounts of real input data may imply a subjectivity of the analysis. Further testing needs to be done to prove universal applicability. In this regard, the precision vs. recall trade-off of the software is required to be further investigated to determine ratios between false positives and false negatives. Additionally, time-lapse data should be featured not only in the GUI but in the analysis as well. Since the project was conducted, the computational capabilities of embedded hardware have dramatically improved. Future adoptions of this work should therefore utilize state-of-the-art embedded hardware and software packages.

In general, the presented biosensor represents a proof of concept of a modular whole-cell, point-of-contact biosensing system. It enables rapid and inexpensive detection of *P. aeruginosa*,

providing intuitive feedback through integrated, real-time analysis. The applicability of this sensor platform in other fields, such as food, water, and environmental safety, offers further innovation potential.

Acknowledgements

Contributions

Experiments were performed by the "iGEM Team Aachen 2014" members, namely, Vera Alexandrova, Nina Bailly, Philipp Demling, Florian Gohr, René Hanke, Markus Joppich, Ansgar Niemöller, Patrick Opdensteinen, Michael Osthege, Björn Peeters, Julia Plum, Stefan Reinhold, Anna Schechtel, Eshani Sood, and Arne Zimmermann. The team was advised by Suresh Sudarsan and Ljubica Vojcic and instructed by Lars Blank, Wolfgang Wiechert, and Ulrich Schwaneberg. The chapter was written by (alphabetically) Nina Bailly, Philipp Demling, Florian Gohr, René Hanke, Patrick Opdensteinen, and Michael Osthege. Markus Joppich, Suresh Sudarsan, Ulrich Schwaneberg, Lars Blank, and Wolfgang Wiechert reviewed this chapter.

Author details

René Hanke[1,†*], Nina Bailly[1,†], Philipp Demling[1,†], Florian N. Gohr[1,†], Patrick Opdensteinen[1,†], Michael J. Osthege[1,†], Markus Joppich[1], Suresh Sudarsan[2], Ulrich Schwaneberg[3], Wolfgang Wiechert[4] and Lars M. Blank[2]

*Address all correspondence to: rene.hanke@rwth-aachen.de

1 iGEM Team Aachen 2014, RWTH Aachen University, Aachen, Germany

2 Institute of Applied Microbiology, RWTH Aachen University, Aachen, Germany

3 Institute of Biotechnology, RWTH Aachen University, Aachen, Germany

4 Forschungszentrum Jülich GmbH, Institute of Bio- and Geosciences, IBG-1: Biotechnology, Jülich, Germany

† These authors contributed equally to this work

References

[1] Tallury P, Malhotra A, Byrne LM, Santra S. Nanobioimaging and sensing of infectious diseases. Advanced Drug Delivery Reviews. 2010;**62**(4):424-437. DOI: 10.1016/j.addr.2009.11.014

[2] Byrne B, Stack E, Gilmartin N, O'Kennedy R. Antibody-based sensors: Principles, problems and potential for detection of pathogens and associated toxins. Sensors. 2009;**9**(6):4407-4445. DOI: 10.3390/s90604407

[3] Singh R, Das Mukherjee M, Sumana G, Gupta RK, Sood S, Malhotra BD. Biosensors for pathogen detection: A smart approach towards clinical diagnosis. Sensors and Actuators B: Chemical. 2014;**197**:385-404. DOI: 10.1016/j.snb.2014.03.005

[4] Behzadi P, Behzadi E, Ranjbar R. The application of microarray in medicine. ORL.ro. 2014; **7**:24

[5] Lazcka O, Del Campo FJ, Munoz FX. Pathogen detection: A perspective of traditional methods and biosensors. Biosensors and Bioelectronics. 2007;**22**(7):1205-1217. DOI: 10.1016/j. bios.2006.06.036

[6] Ivnitski D, Abdel-Hamid I, Atanasov P, Wilkins E. Biosensors for detection of pathogenic bacteria. Biosensors and Bioelectronics. 1999;**14**(7):599-624. DOI: 10.1016/S0956-5663(99) 00039-1

[7] Rocha-Gaso MI, March-Iborra C, Montoya-Baides A, Arnau-Vives A. Surface generated acoustic wave biosensors for the detection of pathogens: A review. Sensors. 2009;**9**(7): 5740-5769. DOI: 10.3390/s90705740

[8] Zourob M. Biosensor using magnetic particles for pathogen detection. US20170038373 A1. 2015. DOI: 10.3390/s17081704

[9] Montoya A, Ocampo A, March C. Fundamentals of piezoelectric immunosensors. In: Vives AA, editor. Piezoelectric Transducers and Applications. 1st ed. Berlin: Springer; 2009. pp. 289-306. DOI: 10.1007/978-3-540-77508-9_12

[10] Eltzov E, Marks RS. Whole-cell aquatic biosensors. Analytical and Bioanalytical Chemistry. 2011;**400**(4):895-913. DOI: 10.1007/s00216-010-4084-y

[11] iGEM Team Aachen Wiki [Internet]. 2014. Available from: http://2014.igem.org/Team: Aachen/ [Accessed: 2017-10-28]

[12] Wu L, Estrada O, Zaborina O, Bains M, Shen L, Kohler JE, et al. Recognition of host immune activation by *Pseudomonas aeruginosa*. Science. 2005;**309**(5735):774-777. DOI: 10.1126/ science.1112422

[13] de Bentzmann S, Plésiat P. The *Pseudomonas aeruginosa* opportunistic pathogen and human infections. Environmental Microbiology. 2011;**13**(7):1655-1665. DOI: 10.1111/ j.1462-2920.2011.02469.x

[14] Nadal Jimenez P, Koch G, Thompson JA, Xavier KB, Cool RH, Quax WJ. The multiple signaling systems regulating virulence in *Pseudomonas aeruginosa*. Microbiology and Molecular Biology Reviews. 2012;**76**(1):46-65. DOI: 10.1128/MMBR.05007-11

[15] Ng WL, Bassler BL. Bacterial quorum-sensing network architectures. Annual Review of Genetics. 2015;**43**:197-222. DOI: 10.1146/annurev-genet-102108-134304

[16] Li YH, Tian X. Quorum sensing and bacterial social interactions in biofilms. Sensors. 2012;**12**:2519-2538. DOI: 10.3390/s120302519

[17] Waters CM, Bassler BL. Quorum sensing: Cell-to-cell communication in bacteria. Annual Review of Cell and Developmental Biology. 2005;**21**(1):319-346. DOI: 10.1146/annurev. cellbio.21.012704.131001

[18] Latifi A, Foglino M, Tanaka K, Williams P, Lazdunski A. A hierarchical quorum-sensing cascade in *Pseudomonas aeruginosa* links the transcriptional activators LasR and RhIR (VsmR) to expression of the stationary-phase sigma factor RpoS. Molecular Microbiology. 1996;**21**(6):1137-1146. DOI: 10.1046/j.1365-2958.1996.00063.x

[19] Broussard JA, Rappaz B, Webb DJ, Brown CM. Fluorescence resonance energy transfer microscopy as demonstrated by measuring the activation of the serine/threonine kinase Akt. Nature Protocols. 2013;**8**(2):265-281. DOI: 10.1038/nprot.2012.147

[20] Ganesan S, Ameer-beg SM, Ng TTC, Vojnovic B, Wouters FS. A dark yellow fluorescent protein (YFP)-based resonance energy-accepting chromoprotein (REACh) for Förster resonance energy transfer with GFP. Proceedings of the National Academy of Sciences of the United States of America. 2006;**103**(11):4089-4094. DOI: 10.1073/pnas.0509922103

[21] Cormack BP, Valdivia RH, Falkow S. FACS-optimized mutants of the green fluorescent protein (GFP). Gene. 1996;**173**(1):33-38. DOI: 10.1016/0378-1119(95)00685-0

[22] Van Der Meer BW, Coker G, Chen SYS. Resonance Energy Transfer: Theory and Data. 1st ed. Weinheim: Wiley-VCH; 1994

[23] Kapust RB, Tözsér J, Fox JD, Anderson DE, Cherry S, Copeland TD. Tobacco etch virus protease: Mechanism of autolysis and rational design of stable mutants with wild-type catalytic proficiency. Protein Engineering. 2001;**14**(12):993-1000. DOI: 10.1093/protein/14.12.993

[24] Shetty R. pSB3K3 Vector Backbone Specification [Internet]. 2004. Available from: http://parts.igem.org/Part:pSB3K3. [Accessed: 2017-10-28]

[25] Che A. pSB1C3 Vector Backbone Specification [Internet]. 2008. Available from: http://parts.igem.org/Part:pSB1C3. [Accessed: 2017-10-28].

[26] Mallick N. Biotechnological potential of immobilized algae for wastewater N, P and metal removal: A review. Biometals. 2002;**15**(4):377-390. DOI: 10.1023/A:1020238520948

[27] Nilsson K, Birnbaum S, Flygare S, Linse L, Schröder U, Jeppsson U, et al. A general method for the immobilization of cells with preserved viability. Applied Microbiology and Biotechnology. 1983;**17**(6):319-326. DOI: 10.1007/BF00499497

[28] Leenen EJTM, Dos Santos VAP, Grolle KCF, Tramper J, Wijffels R. Characteristics of and selection criteria for support materials for cell immobilization in wastewater treatment. Water Research. 1996;**30**(12):2985-2996. DOI: 10.1016/S0043-1354(96)00209-6

[29] Stricker J, Maddox P, Salmon ED, Erickson HP. Rapid assembly dynamics of the *Escherichia coli* FtsZ-ring demonstrated by fluorescence recovery after photobleaching. Proceedings of the National Academy of Sciences of the United States of America. 2002;**99**(5):3171-3175. DOI: 10.1073/pnas.052595099

[30] Nock R, Nielsen F. Statistical region merging. IEEE Transactions on Pattern Analysis and Machine Intelligence. 2004;**26**(11):1452-1458. DOI: 10.1109/TPAMI.2004.110

[31] Joppich M, Rausch D, Kuhlen T. Adaptive human motion prediction using multiple model approaches. Virtuelle und Erweiterte Realität 10. Work. der Gi-fachgr. VR/AR. 2013; 169-180.

[32] iGEM Team Aachen Wiki [Internet]. 2014. Available from: http://2014.igem.org/Team:Aachen/ Project/Measurement_Device#watsonmeasurarty. [Accessed: 2017-10-28]

[33] Lee CS, Wetzel K, Buckley T, Wozniak D, Lee J. Rapid and sensitive detection of *Pseudomonas aeruginosa* in chlorinated water and aerosols targeting gyrB gene using real-time PCR. Journal of Applied Microbiology. 2011;**111**(4):893-903. DOI: 10.1111/j.1365-2672.2011. 05107.x

[34] Mohammadi Kouchesfahani M, Alimohammadi M, Nabizadeh Nodehi R, Aslani H, Rezaie S, Asadian S. *Pseudomonas aeruginosa* and heterotrophic bacteria count in bottled waters in Iran. Iranian Journal of Public Health. 2015;**44**(11):1514-1519

[35] Brett MM, Ghoneim AT, Littlewood JM, Losowsky MS. Development of enzyme linked immunosorbent assay (ELISA) to detect antibodies to *Pseudomonas aeruginosa* cell surface antigens in sera of patients with cystic fibrosis. Journal of Clinical Pathology. 1986;**39**(10):1124-1129. DOI: 10.1136/jcp.39.10.1124

[36] He F, Liu S. Detection of *P. aeruginosa* using nano-structured electrode-separated piezoelectric DNA biosensor. Talanta. 2004;**62**(2):271-277. DOI: 10.1016/j.talanta.2003.07.007

[37] Tokonami S, Nakadoi Y, Takahashi M, Ikemizu M, Kadoma T, Saimatsu K, et al. Label-free and selective bacteria detection using a film with transferred bacterial configuration. Analytical Chemistry. 2013;**85**(10):4925-4929. DOI: 10.1021/ac3034618

[38] Žukovskaja O, Jahn IJ, Weber K, Cialla-May D, Popp J. Detection of *Pseudomonas aeruginosa* metabolite pyocyanin in water and saliva by employing the SERS technique. Sensors. 2017;**17**(8):1704. DOI: 10.3390/s17081704

[39] Ahmed A, Rushworth JV, Hirst NA, Millner PA. Biosensors for whole-cell bacterial detection. Clinical Microbiology Reviews. 2014;**27**(3):631-646. DOI: 10.1128/CMR.00120-13

[40] Struss A, Pasini P, Ensor CM, Raut N, Daunert S. Paper strip whole cell biosensors: A portable test for the semiquantitative detection of bacterial quorum signaling molecules. Analytical Chemistry. 2010;**82**(11):4457-4463. DOI: 10.1021/ac100231a

[41]   Melamed S, Elad T, Belkin S. Microbial sensor cell arrays. Current Opinion in Biotechnology. 2012;**23**(1):2-8. DOI: 10.1016/j.copbio.2011.11.024

[42]   Kim K, Lee BU, Hwang GB, Lee JH, Kim S. Drop-on-demand patterning of bacterial cells using pulsed jet electrospraying. Analytical Chemistry. 2010;**82**(5):2109-2112. DOI: 10.1021/ac9027966

[43]   Merrin J, Leibler S, Chuang JS. Printing multistrain bacterial patterns with a piezoelectric inkjet printer. PLoS One. 2007;**2**(7):e663. DOI: 10.1371/journal.pone.0000663

[44]   iGEM Team Aachen Wiki [Internet]. 2014. Available from: http://2014.igem.org/Team: Aachen/Attributions. [Accessed: 2017-10-28]